

Cooperative Multi-Robot Systems

A study of Vision-based 3-D Mapping using Information Theory

Rui Rocha^{*†}, Jorge Dias^{*} and Adriano Carvalho[†]

{*rprocha | jorge*}@*isr.uc.pt*, *asc@fe.up.pt*

^{*}Institute of Systems and Robotics
Faculty of Sciences and Technology, Univ. of Coimbra
Pinhal de Marrocos, 3030-290 Coimbra, PORTUGAL

[†]Department of Electrical and Computer Engineering
Faculty of Engineering, University of Porto
Rua Dr. Roberto Frias, 4200-465 Porto, PORTUGAL

Abstract—Building cooperatively 3-D maps of unknown environments is one of the application fields of multi-robot systems. This article introduces a distributed architecture, within a probabilistic framework for vision-based 3-D mapping, whereby each robot is committed to cooperate with other robots through information sharing. An entropy-based measure of information utility is defined, which a robot uses for communicating to its teammates the most useful measurements, thus preventing the robot to overwhelm communication resources with redundant information. Experiments with real robots, equipped with stereo-vision, yielded important conclusions about the way robots should cooperate on sharing information.

Index Terms—Cooperative multi-robot systems, 3-D mapping, entropy, information utility, communication.

I. INTRODUCTION

Multi-robot systems (MRS) have been widely investigated for the last decade [1]. These systems employ teams of cooperative robots to carry out missions that either cannot be achieved by a single robot, or where a multi-robot solution is more efficient, cost effective, reliable and robust than a single robot. Building a 3-D map of an unknown environment is one of the application fields of MRS.

Robotic mapping addresses the problem of acquiring spatial models of physical environments through mobile robots [2], using range sensors such as cameras or laser range finders. As sensors have always limited range, are subject to occlusions and yield measurements with noise, mobile robots have to navigate through the environment and build the map iteratively. Robots can be used for building fastidious maps of indoor environments [3], but they are particularly useful on mapping missions of hazardous environments for human beings, such as abandoned underground mines [4] or nuclear facilities [5]. Although it is recognized the potential of MRS on such mapping missions, most of the current state-of-the-art of robot mapping is restricted to single robot solutions, with some exceptions mainly focused on exploration and coordination [6], [7], [8]. Extensive research has been devoted to SLAM (e.g. [4]), i.e. the problem of building a map and simultaneously tracking the robot's position on that map. In this article, it is assumed that robots are externally localized, so the work here presented does not fall in the heading of SLAM or localization.

Most of the work in MRS has been devoted to the definition of different architectures, mostly behavior-based, that rule the interaction between the behaviors of individual robots [6], [9], [10], [8]. Communication is a central issue of MRS because it determines the possible modes of interaction among robots. As communication is always limited, either in resources applied to perceive the world or in bandwidth of a communication channel, using efficiently those resources is crucial to scale up cooperative architectures for teams of many robots, without limiting them to simple reactive and loosely-cooperative systems, with very limited or no awareness. Although previous work on communication structures for MRS has led to some useful conclusions and design guidelines [11], [12], [13], [14], there is no a principled formalism that can be systematically used to share efficiently sensory data based on information utility assessment. Current architectures extensively use explicit communication, not taking care [6], [9], giving low emphasis [8], or using no principled heuristics to avoid the communication of redundant information. An exception is [10], where entropy is used to define theoretic information measures for predicting the expected information outcome associated with control actions. However, it is mainly focused on coordination and it is not clear how it can be used to share efficiently sensory data within mapping missions.

In [15], we refine coverage maps [3] to develop a grid-based probabilistic model of a 3-D map (see a summary in section 2), which provides a compact representation of the coverage (occupancy) of each cell and a straightforward Bayesian update procedure. In section 3, we use this model to present a distributed architecture model for 3-D mapping with a team of cooperative mobile robots. In section 4, we propose an information-theoretic measure of information utility, which is used by robots to cooperate through sharing sensory data, with an efficient use of communication resources. Section 5 presents an experimental setup with cooperative mobile robots equipped with stereo-vision range sensors, which was used for carrying out a set of 3-D mapping experiments. Results yielded by those experiments are used to highlight the benefits provided by cooperation and the influence of information selectivity on the team's performance. The article ends with conclusions and future work.

II. PROBABILISTIC FRAMEWORK FOR 3-D MAPS

This section summarizes the probabilistic framework for 3-D maps developed in [15]. Hereafter, vectors are written with bold lower case letters; tuples and sets are both written with upper case letters, but sets are written in calligraphy. The index $k \in \mathbb{N}_0$ is used for batches of measurements. The set of time instants when measurements are obtained is $\mathcal{T} = \{t_k : t_k \in \mathbb{R}, k \in \mathbb{N}\}$, with $t_{k-1} \leq t_k, \forall k \in \mathbb{N}$. The k -th batch of measurements is obtained at time instant $t = t_k$. The index $k = 0$ denotes the initial time instant $t = t_0 \leq t_k, \forall k \in \mathbb{N}$, before any measurements.

A. Batches of measurements

A range sensor, a stereo-vision sensor in our case, typically provides batches of distance measurements from its location. The k -th batch of measurements is the tuple $M_k = (\mathbf{x}_k, \mathcal{V}_k)$, being $\mathcal{V}_k = \{\vec{\mathbf{v}}_{k,i} \in \mathbb{R}^3 : i \in \mathbb{N}, i \leq m_k\}$ a set of m_k applied vectors (measurements), connecting the 3-D point \mathbf{x}_k , where the robot's sensor is located, to the set of points $\{\mathbf{x}_k + \vec{\mathbf{v}}_{k,i} : i \in \mathbb{N}, i \leq m_k\}$, where obstacles are detected. The index i is the index for measurements within a given batch of measurements. The sequence of batches of measurements up to the k -th batch of measurements, corresponding to the period of time $t_0 \leq t \leq t_k$, is the set $\mathcal{M}_k = \{M_b : b \in \mathbb{N}, b \leq k\}$. Before any batch of measurements, i.e. for $k = 0$, the sequence of batches is the empty set $\mathcal{M}_0 = \emptyset$. The k -th batch of measurements sent to other robots is $S_k = (\mathbf{x}_k, \mathcal{U}_k)$, $\mathcal{U}_k \subseteq \mathcal{V}_k$, being \mathcal{U}_k a set s_k of useful measurements. The k -th batch of measurements received from other robots is $R_k = (\mathbf{x}'_k, \mathcal{U}'_k)$, being \mathcal{U}'_k a set of r_k useful measurements from the sensor of other robot, whose pose is \mathbf{x}'_k .

B. 3-D volumetric map

The 3-D workspace is divided into equal sized voxels (cells) with edge e , $e \in \mathbb{R}$, and volume e^3 . The set of all voxels yielded by such division is the 3-D grid \mathcal{Y} and the index l is used for denoting individual voxels. The coverage of a voxel $l \in \mathcal{Y}$ is the portion of its volume which is covered (occupied) by obstacles and is represented through the random variable C_l , taking values $c_l \in [0, 1]$. The index j is used for measurements influencing the coverage estimate of a given voxel. Given a batch of measurements $M_k = (\mathbf{x}_k, \mathcal{V}_k)$, the set of influenced voxels by a measurement $\vec{\mathbf{v}}_{k,i} \in \mathcal{V}_k$ is denoted as $\mathcal{Z}_{k,i} \subset \mathcal{Y}$. An individual measurement influencing the coverage estimate of a voxel $l \in \mathcal{Y}$ is the tuple $D_j^l = (d_j, d_j^l)$, being $d_j \in \mathbb{R}$ the distance between the sensor and the detected obstacle and $d_j^l \in \mathbb{R}$ the distance between the sensor and the voxel's center. The set of measurements influencing the coverage estimate of a voxel $l \in \mathcal{Y}$, after k batches of measurements, is $\mathcal{D}_k^l = \{D_j^l : j \in \mathbb{N}, j \leq n_k(l)\}$ and has cardinality $n_k(l) \in \mathbb{N}_0$. Before any batch of measurements, the set of influencing measurements is the empty set $\mathcal{D}_0^l = \emptyset$. The coverage probability density function (pdf) of a voxel $l \in \mathcal{Y}$, after k batches of measurements, is $p(c_l | \mathcal{M}_k) = p(c_l | \mathcal{D}_k^l)$. The 3-D probabilistic coverage map, after k batches of measurements, is the set of pdf $\mathcal{P}(\mathcal{C} | \mathcal{M}_k) = \{p(c_l |$

$\mathcal{M}_k) : l \in \mathcal{Y}\}$, being $\mathcal{C} = \{C_l : l \in \mathcal{Y}\}$ a set of coverage random variables having one element for each voxel $l \in \mathcal{Y}$. Before any batch of measurements, the initial map is denoted as $\mathcal{P}(\mathcal{C} | \mathcal{M}_0) = \{p(c_l | \mathcal{M}_0) = p(c_l | \mathcal{D}_0^l) : l \in \mathcal{Y}\}$.

C. Surveying the environment

The robot's pose as a function of time is the tuple $Y(t) = (\mathbf{x}(t), \mathbf{a}(t))$, $\mathbf{x}(t), \mathbf{a}(t) \in \mathbb{R}^3$, being $\mathbf{x}(t)$ the sensor's position and $\mathbf{a}(t)$ its attitude (three Euler angles). The robot's pose for the k -th batch of measurements is $Y_k = (\mathbf{x}_k, \mathbf{a}_k)$. The robot follows an entropy gradient-based survey strategy for selecting its next viewpoint Y^s , given its current map. All coordinates refer to a global coordinates frame $\{W\}$.

III. DISTRIBUTED ARCHITECTURE FOR 3-D MAPPING

In this section, we introduce a distributed architecture for performing 3-D mapping missions with a cooperative multi-robot system. Figures 1 and 2 depict complementary views of the architecture. Although individual robots belonging to the multi-robot system might be heterogeneous in terms of sensory skills and mobility, all of them follow the same architecture model when performing the 3-D mapping mission. That's why both figures refer to an individual robot; nevertheless, the interaction with other robots is represented through the communication block and its associated data flow.

Figure 1 shows the different parts of the process and how they interact. The robot's platform is assumed to have a sensor, a localization module and an actuator. The sensor provides new sets of vectors \mathcal{V}_{k+1} where obstacles are detected from the current sensor's pose $Y(t)$. The localization module gives the sensor's pose $Y(t)$, including position and attitude. The actuator changes the sensor's pose (robot's pose) accordingly with new survey targets Y^s . New data from the robot's sensor is associated with its current pose, given by the localization module, to form a new batch of measurements $M_{k+1} = (\mathbf{x}_{k+1}, \mathcal{V}_{k+1})$. Then, index k is incremented and the new batch of measurements becomes the current batch M_k . The memory of measurements is updated as $\mathcal{M}_k = \mathcal{M}_{k-1} \cup M_k$. The previous map $\mathcal{P}(\mathcal{C} | \mathcal{M}_{k-1})$ is updated upon the new batch of measurements M_k , which yields the current map $\mathcal{P}(\mathcal{C} | \mathcal{M}_k)$. The current map is used to choose a new target pose Y^s which is the reference input to the robot's actuator. As part of map updating, it is built a batch of measurements $S_k = (\mathbf{x}_k, \mathcal{U}_k)$ having the most useful data from sensor $\mathcal{U}_k \subseteq \mathcal{V}_k$. Those selected measurements are shared with other robots through the communication module. This module can also provide the robot with batches of measurements $R_k = (\mathbf{x}'_k, \mathcal{U}'_k)$ given by other robots and the map is updated accordingly. Cooperation among robots arises because of this altruistic commitment to share useful measurements.

Figure 2 depicts a flowchart showing the sequence of the aforementioned robot's operations and interactions. At the beginning of the mission, an initial map is given to the robot. Then it gets a new batch of measurements, updates the map and shares useful measurements with other robots. Then it might receive measurements from other robots and, in that

distribution of sensors makes possible to reduce the map’s uncertainty more quickly than if a single robot is used; (ii) *reliability and robustness* – with redundancy in robots capabilities, the failure of any particular robot does not necessarily compromise the overall mission success; (iii) *specialization* – robots with different sensory or motion skills may have complementary and specialized features that overcome their individual limitations and increase the team’s total utility.

We assume that each robot, besides being able to build and update its own local 3-D map based on information from its own sensors, is also committed to share new acquired sensory information with its teammates through communication. Whenever a given robot gets a batch of measurements $M_k = (\mathbf{x}_k, \mathcal{V}_k)$, it sends to the other robots a sub-set of measurements $S_k = (\mathbf{x}_k, \mathcal{U}_k)$. The set

$$\mathcal{U}_k = \{ \vec{\mathbf{u}}_{k,1}, \dots, \vec{\mathbf{u}}_{k,s_k} \} \subseteq \mathcal{V}_k \quad (5)$$

is a set of s_k communicated measurements and \mathbf{x}_k the sensor’s position when those measurements were gathered, which is required for registering those measurements in the local map of other robots. When a robot receives a batch of communicated measurements $R_k = (\mathbf{x}'_k, \mathcal{U}'_k)$, it updates its local map as if measurements \mathcal{U}'_k would have been gathered by its own sensor when located at position \mathbf{x}'_k .

As communication channels have always limited capacity, when a robot is acting as information provider, it has to limit the amount of communicated data and select the most useful measurements gathered from its own sensors. On doing it, the robot uses equation (3) to assess the information utility associated with the measurements \mathcal{V}_k and classifies them by utility. Let define $\max(s_k)$ as being the maximum number of allowable communicated measurements at a given time instant. Let also define I_{min} as being the minimum allowable information utility for a communicated measurement. The set (5) is built in such a way that the proposition

$$\begin{aligned} s_k &\leq \max(s_k) \wedge \\ s_k &< \max(s_k) \Rightarrow \forall \vec{\mathbf{v}}_{k,z} \in \mathcal{V}_k \setminus \mathcal{U}_k, I_{k,z} < I_{min} \wedge \\ \forall \vec{\mathbf{u}}_{k,j} \in \mathcal{U}_k, I_{k,j} &\geq I_{min} \wedge \forall \vec{\mathbf{v}}_{k,w} \in \mathcal{V}_k \setminus \mathcal{U}_k, I_{k,w} \leq I_{k,j} \end{aligned} \quad (6)$$

is true. The proposition is true (the set of communicated measurements is valid) if the following conditions are met: (a) the size of the set is not greater than $\max(s_k)$; (b) the size of the set is less than $\max(s_k)$ only if it includes all measurements in the set \mathcal{V}_k having an information utility not less than I_{min} ; (c) the information utility of communicated measurements is at least I_{min} and all not communicated measurements have lower or equal utility than those which are selected to be communicated.

V. EXPERIMENTS WITH REAL ROBOTS

The 3-D mapping architecture depicted in figure 1 was used for carrying out a set of experiments in our lab with two Scout robots (see figure 3-a), equipped with a stereo-vision sensor, sonars and wireless communication. Sonars were used for detecting obstacles when moving the platform, and for

preventing a robot to acquire stereo image pairs below a given distance threshold to obstacles. The stereo-vision sensor (see figure 3-b) is a low-cost analog stereo rig, with resolution 160x120 pixels.

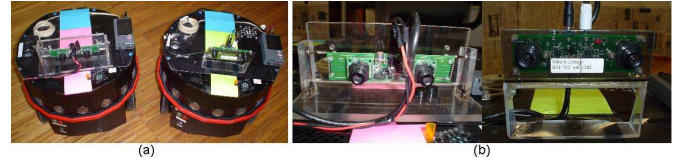


Fig. 3. Mobile robots used on the 3-D mapping experiments: (a) Scout mobile robots from Nomadic Technologies; (b) stereo-vision sensors from Videre Design mounted on the robots. Both robots have colored markers on the top, in order to compute their pose in a global reference frame $\{W\}$, through a RGB camera covering the robots’ workspace and color segmentation.

A. Building 3-D maps with a single robot

In this section, we present and discuss results obtained within a 3-D mapping mission using a single robot. The 3-D mapping experiment was carried out until the map’s entropy, computed through (2), had been reduced below a given predefined threshold h_{th} . This stopping criteria has an important associated performance measure of the 3-D mapping mission, which is the first time instant $t_{k_{max}}$ when it is achieved. This time instant verifies the proposition

$$h(t_{k_{max}}) \leq h_{th} \wedge \forall k < k_{max}, h(t_k) > h_{th} \quad (7)$$

and is associated with the k_{max} -th set of measurements. In our study, we used an initial map where every voxels $l \in \mathcal{Y}$ had an initial Gaussian $p(c_l | \mathcal{D}_0^l)$ with $\sigma_l = 10.0$ which, given the workspace parameters for which the maps were built, corresponded to an initial map’s entropy $h(0) = 9.922 \times 10^4$. The stopping criteria $h_{th} = 0$ was used, which corresponded, for example, to a final map having Gaussians with $\sigma_l = 0.242$ for the coverage belief of every voxels $l \in \mathcal{Y}$.

The robot needed $t_{k_{max}} = 9053$ s to accomplish the mission. The robot gathered a total of $k_{max} = 303$ batches of measurements, with an average size of $\overline{m_k} = 9049$ measurements. Figure 4 shows the graph of the map’s entropy $h(t)$ along the mission. The symmetric of its first derivative measures information gain, therefore the graph shows that measurements obtained by the beginning of the mission are the most informative (useful) and that measurements’ utility decreases as long as the mission is executed. The curve also shows that a decrease of the threshold h_{th} has a strong impact in $t_{k_{max}}$. Dashed lines in figure 4 show an example where $t_{k_{max}}$ increased 914.4%.

B. Building 3-D maps with a team of cooperative robots

This section presents experiments carried with a team of two cooperative mobile robots (see Figure 3), using different values for the information sharing parameters $\max(s_k)$ and I_{min} . Figure 5 depicts an example of each robot’s map at the end of a 3-D mapping mission. Table I summarizes the results obtained with the two cooperative mobile robots. The

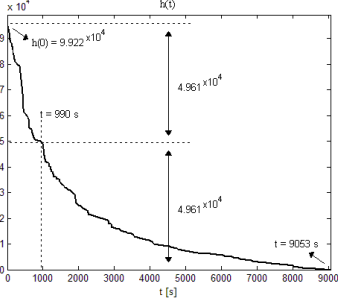


Fig. 4. Map's entropy along a 3-D mapping mission with a single robot.

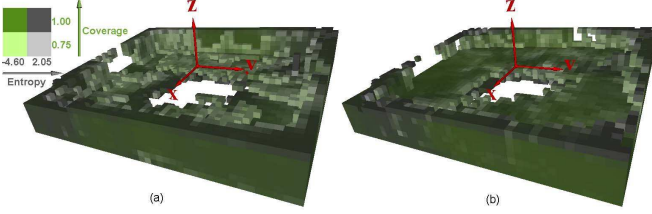


Fig. 5. Map of each robot at the end of a 3-D mapping mission with two cooperative mobile robots. For the presented case, the parameters $\max(s_k) = 20000$ and $I_{min} = 0.1520$ were used. The best map is the one on the right of the figure, which means that the respective robot reached $h_{th} = 0$ first.

4th column shows the ratio between the mission execution time t_{kmax} with two robots and with one robot t_{kmax}^1 . Given that our voxels' coverage belief were always Gaussians, the values used for I_{min} , $\{0, 0.00723, 0.01450, 0.07400, 0.15200, 0.32193\}$, mean an average reduction on the standard deviation of the influenced voxels by a measurement of at least $\{0\%, 0.5\%, 1\%, 5\%, 10\%, 20\%\}$, respectively. Recall that when a robot acquires a new batch of m_k measurements $M_k = (\mathbf{x}_k, \mathcal{V}_k)$ through its own sensor, it might sent to the other robot a batch of s_k useful measurements $S_k = (\mathbf{x}_k, \mathcal{U}_k)$, with $s_k \leq m_k \wedge s_k \leq \max(s_k) \wedge r_k = 0$. Conversely, a k -th batch of m_k measurements $M_k = (\mathbf{x}_k, \mathcal{V}_k)$ might not be acquired from its own sensor and thus might be a batch of r_k measurements sent (shared) by the other robot $M_k = R_k = (\mathbf{x}'_k, \mathcal{U}'_k)$, with $r_k = m_k \leq \max(s_k) \wedge s_k = 0$. The 5th column is the total number of measurements m_T gathered by a robot along the mission, which is given by

$$m_T = \sum_{k=1}^{k_{max}} m_k. \quad (8)$$

The last column shows the total number of received measurements from other robot(s) r_T , which is computed through

$$r_T = \sum_{k=1}^{k_{max}} r_k. \quad (9)$$

1) *Advantages provided by cooperation:* The graph on the left of figure 6 compares the map's entropy $h(t)$ for the single robot case and for the fastest experiment with two robots (4th row of table I). The cooperation between the

TABLE I

RESULTS OBTAINED WITHIN THE EXPERIMENTS WITH TWO ROBOTS.

$\max(s_k)$	I_{min}	t_{kmax}	$\frac{t_{kmax}}{t_{kmax}^1}$	m_T	r_T	
500	0.01450	8483	0.94	2795351	74729	3 %
1000	0.01450	8387	0.93	2726837	135661	5 %
1750	0.01450	7332	0.81	2447091	184550	8 %
2500	0.01450	6530	0.72	2375273	207636	9 %
5000	0.01450	7955	0.88	2643728	271612	10 %
20000	0	9450	1.04	3192788	1134455	36 %
20000	0.00723	7563	0.84	2453021	457390	19 %
20000	0.01450	6571	0.73	2345844	332270	14 %
20000	0.07400	7007	0.77	2676612	128345	5 %
20000	0.15200	7301	0.81	2595398	59499	2 %
20000	0.32193	7727	0.85	2930155	27323	1 %

two robots accelerated the reduction of the map's entropy and led to a reduction of 28% in t_{kmax} . As robots share useful measurements through communication, each robot is able to integrate in its map a greater number of measurements per time unit (see the graph on the right of the figure 6) and achieves a faster reduction of its maps' entropy. The graph on the right of figure 6 shows that although the two values of m_T were similar, measurements were obtained within time intervals t_{kmax} quite different. Besides enabling

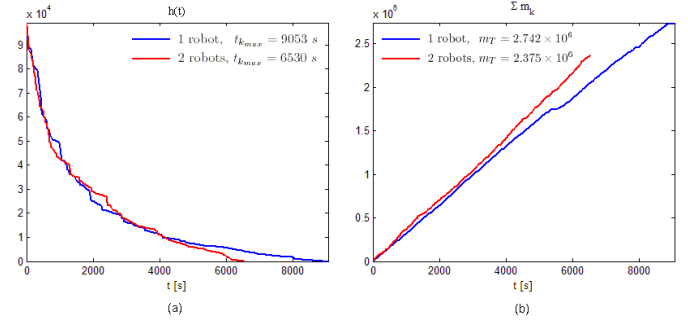


Fig. 6. Comparison of a 3-D mapping mission using a single robot or two robots: (a) map's entropy along the mission; (b) number of integrated measurements into the map. For the presented two robots case, $\max(s_k) = 2500$ and $I_{min} = 0.0145$.

cooperation and its aforementioned benefits, the coexistence of several robots in the same workspace and the communication among robots also yield some pitfalls contributing for the degradation of the team's overall performance: (a) robots must share the workspace which leads to some mutual interference; (b) the time spent on communicating measurements to other robots sometimes delays operations; (c) the time required for processing received measurements through communication and updating the map upon them might not be negligible. Minimizing the aforementioned undesirable effects is a key factor for taking the maximum advantage from the cooperation among robots and this is the main issue we will pursue in our future research work.

2) *Influence of communication selectivity:* Figure 7 presents graphs of the ratio t_{kmax}/t_{kmax}^1 and the amount of received measurements $\sum r_k$, for different values of I_{min} and different values of $\max(s_k)$. In figure 7-a, the maximum number of allowable communicated measurements at a given

time instant was $\max(s_k) = 20000$. As the number of measurements yielded by the sensor is about 10^4 measurements, in this situation, $\max(s_k)$ did not restrict the communication for any acquired batch of measurements, because $m_k < \max(s_k)$, $1 \leq k \leq k_{max}$. The graph on the top of figure 7-a shows that decreasing I_{min} from 0.32193 to 0.01450 leads to smaller mission execution times. However, for $I_{min} < 0.01450$, the graph of $t_{k_{max}}$ presents an important inflection, which leads to a fast degradation of the team's performance and puts on evidence the importance of selecting the most useful information to be communicated. If this selection is too weak, most of the communicated information becomes redundant and the time spent on communicating and processing that superfluous information becomes very significant. The curves on the bottom of figure 7-a shows that the derivative at the beginning of the mission is the same because $\max(s_k)$ is common to all of them. However, as long as the mission is executed, the derivative decreases to an extent which depends on the selectivity introduced by the parameter I_{min} .

In figure 7-b, the minimum allowable information utility for a communicated measurement is $I_{min} = 0.01450$. The graph on the top of figure 7-b shows that reducing the communication bandwidth $\max(s_k)$ always leads to an increase of $t_{k_{max}}$ and a poorer team's performance. As cooperation in a 3-D mapping mission relies completely on explicit communication, restricting it also restricts the extent of cooperation. However, in the case of I_{min} , being selective to some extent is beneficial in order to select the most useful information and to avoid the communication of redundant information. The curves on the bottom of figure 7-b shows that the derivative by the end of the mission is the same, because I_{min} is common to all of them, and that it is as high as $\max(s_k)$ at the start.

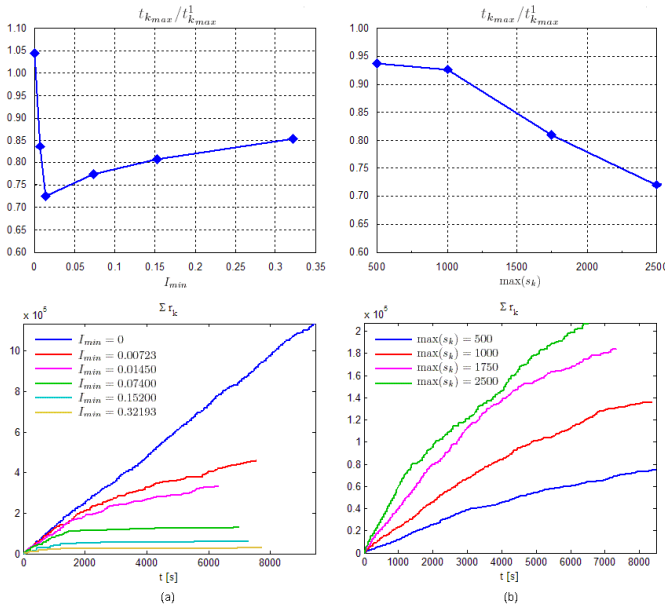


Fig. 7. Influence of I_{min} and $\max(s_k)$ on the ratio $t_{k_{max}}/t_{k_{max}}^1$ (top) and on $\sum r_k$ (bottom): (a) different values of I_{min} and $\max(s_k) = 20000$; (b) different values of $\max(s_k)$ and $I_{min} = 0.01450$.

These results yield some guidelines for developing communication schemes aiming at fostering cooperation. While $\max(s_k)$ is imposed by the communication channel capacity, I_{min} has to be tuned in an intelligent way, whereby its selective power is beneficial for the robotic team's performance. It should be either selective enough to avoid communicating redundant information and not too selective, enabling efficient information sharing and cooperation among robots.

VI. SUMMARY AND CONCLUSIONS

This article presented a 3-D mapping distributed architecture, which enables to share efficiently sensory data in a team of cooperative mobile robots, using an entropy-based measure of information utility. Experimental results of 3-D mapping experiments with real robots, equipped with on-board stereo-vision, were presented and discussed. We showed that a cooperative multi-robot system allows to accomplish the mission in less time. Obtained results also yielded important guidelines for future development of communication schemes within multi-robot systems. Future work will focus on extending current robots' cooperation framework with an exploration coordination method for minimizing the robots' interference.

REFERENCES

- [1] T. Arai, E. Pagello, and L. Parker. Special issue on advances in multirobot systems. *IEEE Tr. on Rob. and Autom.*, 18(5):655–864, 2002.
- [2] S. Thrun. Robotic mapping: a survey. In G. Lakemeyer and B. Nebel, editors, *Exploring Artificial Intelligence in the New Millenium*. Morgan Kaufmann, 2002.
- [3] C. Stachniss and W. Burgard. Mapping and exploration with mobile robots using coverage maps. In *Proc. of IEEE/RSJ Int. Conf. on Intelligent Robots and Systems (IROS'2003)*, pages 467–472, 2003.
- [4] S. Thrun, D. Hahnel, D. Ferguson, M. Montermelo, R. Riebwel, W. Burgard, C. Baker, Z. Omohundro, S. Thayer, and W. Whittaker. A system for volumetric robotic mapping of underground mines. In *Proc. of IEEE Int. Conf. on Robotics and Automation (ICRA'03)*, 2003.
- [5] M. Maimone, L. Matthies, J. Osborn, E. Rollins, J. Teza, and S. Thayer. A photo-realistic 3-D mapping system for extreme nuclear environments: Chernobyl. In *Proc. of IEEE/RSJ Int. Workshop on Intelligent Robots and Systems (IROS'98)*, volume 3, pages 1521–1527, 1998.
- [6] B. Yamauchi. Frontier-based exploration using multiple robots. In *Proc. of 2nd Int. Conf. on Autonomous Agents*, pages 47–53, 1998.
- [7] W. Burgard, M. Moors, D. Fox, R. Simmons, and S. Thrun. Collaborative multi-robot exploration. In *Proc. of IEEE Int. Conf. on Robotics and Automation (ICRA'00)*, volume 1, pages 476–481, 2000.
- [8] K. Konolige, D. Fox, C. Ortiz, A. Agno, M. Eriksen, B. Limketkai, J. Ko, B. Morisset, D. Schutz, B. Stewart, and R. Vincet. Centibots: very large scale distributed robotic teams. In *Proc. of Int. Symp. on Experimental Robotics, Singapore*, 2004.
- [9] L. Parker. ALLIANCE: An architecture for fault-tolerant multi-robot cooperation. *IEEE Tr. on Rob. and Automation*, 14(2):220–240, 1998.
- [10] B. Grocholsky, A. Makarenko, and H. Durrant-Whyte. Information-theoretic coordinated control of multiple sensor platforms. In *Proc. of Int. Conf. on Intelligent Robots and Systems*, pages 1521–1526, 2003.
- [11] R. Arkin. Cooperation without communication: Multi-agent schema based robot navigation. *Journal of Robotic Systems*, 9(3):351–364, 1992.
- [12] T. Balch and R. Arkin. Communication in reactive multiagent robotic systems. *Autonomous Robots*, 1(1):27–52, 1994.
- [13] M. Tambe. Towards flexible teamwork. *Journal of Artificial Intelligence Research*, 7:83–124, 1997.
- [14] P. Stone and M. Veloso. Task decomposition, dynamic role assignment, and low-bandwidth communication for real-time strategic teamwork. *Artificial Intelligence*, 110(2):241–273, 1999.
- [15] R. Rocha, J. Dias, and A. Carvalho. Entropy-based 3-D mapping with teams of cooperative mobile robots: a simulation study. Technical report, ISR, University of Coimbra, Portugal, Feb. 2004. http://thor.deec.uc.pt/~rprocha/publications/040209_techReport2.pdf.